

Saturation-based robustly optimal hierarchical operation control of microgrids

Ujjwal Pratap* Steffen Hofmann**

* *Automation and Sensorics in Networked Systems, University of Kassel, Germany, (e-mail: ujjwal.pratap@uni-kassel.de).*

** *TU Berlin, Germany, (e-mail: steffen.hofmann@tu-berlin.de)*

Abstract: This paper studies the problem of robustly optimal operation control of microgrids with a high share of renewable energy sources. The main goal is to ensure optimal operation under a wide range of circumstances, given the highly intermittent and uncertain nature of renewable sources and load demand. We formally state this problem, and, in order to solve it, we make effective use of the hierarchical power system control approach. We consider an enhanced primary control layer including droop control and autonomous limitation of power and energy. We prove that this enables the use of constant power setpoints to achieve optimal operation under certain conditions. In order to relax these conditions, the approach is combined with an energy management system, which solves a robust unit commitment problem within a model predictive control framework. Finally, a case study demonstrates the viability of the control design.

Keywords: Operation control, energy management systems, hierarchical control, microgrids

1. INTRODUCTION

Energy production is shifting from conventional generators to inverter-interfaced renewable energy sources (RES), worldwide. Many RES installations work in grid-following mode, which implies that they synchronize their output frequency to the observed grid frequency and inject constant current respectively power into the grid. This can lead to a situation where there is insufficient capacity of installed grid-forming units for performing frequency and voltage regulation and compensating power imbalances, i.e., power sharing (Rocabert et al., 2012). This is especially true for microgrids (MGs) with high share of RES (Guerrero et al., 2011). It has been proposed (e.g., in Khan et al., 2024) that the path forward involves that RES be increasingly interfaced using grid-forming inverters or inverters with advanced control. However, unlike conventional power sources, RES such as photovoltaic (PV) plants and wind turbines are intermittent, respectively subject to uncertainties. In order to participate in regulation and power sharing, a unit has to be able to vary its power output and thus has to be operated sufficiently far from its physical limitations (Guerrero et al., 2011).

In this paper, we aim at achieving maximum flexibility by allowing that at any point in time only at least one unit is grid-forming, and that any unit can autonomously switch back and forth its role between grid-following and grid-forming. More precisely, we rely on units with grid-forming capabilities to restrict their output power to physical limitations. Implementation of this behavior on the inverter level and related issues such as stability are out of the scope of this paper, but have been the subject of discussion of several contributions (e.g., Du and Lasseter, 2017; Yazdani et al., 2020; Gao et al., 2025) and review papers (e.g., Baeckeland et al., 2024).

In a MG, the energy management system (EMS) provides power set-points to the generation units to fulfil the demand and reduce operating cost. The problem of EMS designs for microgrids has been vastly addressed in the literature, outlining for example the hierarchical control as well as EMS design for scheduling and dispatch under uncertainty (Olivares et al., 2014), both of which are also the main focus of this paper. In this regard, model predictive control (MPC) is one of the popular approaches. It is a receding horizon optimization technique that uses forecasts and can enforce unit constraints (Parisio et al., 2014; Hans et al., 2014). Despite extensive literature on EMS design for MGs (Olivares et al., 2014; Parisio et al., 2014; Schiffer et al., 2016), most approaches tend to overlook explicit consideration of droop control in lower control layers and limiting behavior of units, which might lead to potential mismatch between setpoints and behavior of the lower layers during disturbances and uncertain conditions.

(Hofmann et al., 2021) shows how saturating droop-control can increase overall performance in conjunction with a mini-max MPC-based EMS. In particular, saturating droop increases the set of feasible controls, which in turn can result in a control leading to a lower objective function value. However, a major drawback of mini-max MPC is that only worst-case performance is considered in the objective function. This can lead to wasted potential as the actual realizations of uncertain variables (available renewable power and load demand) are typically not near the worst-case. The motivation of the present paper is to achieve near-optimal performance under all disturbance-scenarios and at the same time simplify the optimization problem. In a related study, (Dörfler et al., 2016) have shown that droop control alone, without interference of an

EMS, can be economically optimal. They mostly consider linear droop functions, but have stated that nonlinear droop functions correspond to optimal controls for more general cost functions; they mention, in particular, that droop curves with deadbands and saturation could correspond to non-smooth and barrier-costs.

In the following, we propose a min-max MPC problem for energy management of MGs, which looks beyond worst-case scenarios of disturbances in renewable generation and load demand, and where the units are droop controlled and include an autonomous power and energy limiting feature. Crucially, local unit controllers are modeled as part of the EMS, including saturation at power and energy limits. By making the EMS aware of these safeguards, it can choose less conservative power setpoints without risking constraint violations. We provide a simplified solution approach based on constant setpoints on the lower layer and a unit commitment problem on the EMS-layer. The remainder of the paper details the system model, description of the optimal control problem, determination of a constant setpoint controller under certain conditions with a formal proof, leading to a hierarchical control structure with a robust EMS which decides a unit commitment problem. Finally, we present a case study to illustrate its performance.

2. MICROGRID MODEL

In this section, we describe the mathematical model of an islanded MG that includes renewable power sharing and takes saturation limits of the units, based on (Hofmann et al., 2021), into account. The model incorporates three types of units, which are conventional units like thermal generators, storage units, RES like wind farms and PV power plants as well as loads. This model, which will be employed in EMS design later in this paper, describes the power output of each unit and accounts for power sharing under saturating conditions. In addition, uncertain renewable generation and load demand is considered which can lead to unit power outputs that differ power setpoints provided by the EMS.

Assumptions: We assume that the primary control ensures a stable operation of the MG and we do not have a secondary control. In addition, we assume that start-up and shut-down times of the conventional units are small compared to the EMS sampling time. Furthermore, we assume that storage losses are negligible compared to the uncertainties introduced by RES and load.

2.1 Preliminaries

\mathbb{R} denotes the set of real numbers and $\mathbb{R}_{\leq 0}$ denotes the set of non-positive real numbers, $\mathbb{R}_{\geq 0}$, the non-negative real numbers and \mathbb{N} denotes the set of positive integers. Operators $\min(x, y)$ and $\max(x, y)$ for the vectors x and y provide the element-wise minimum and maximum respectively. For $x, y \in \mathbb{R}^n$, $x \leq y$ is true if and only if (iff) it is true for all elements. If A and B are matrices of equal dimensions, then $A \leq B$ is true iff it is true for all elements at matching positions. $\mathbf{1}$ is a vector of all ones of appropriate size. $\text{diag}(x)$ is a diagonal matrix, with the elements of the vector x on its diagonal.

Let us denote the saturation of a variable x , with lower and upper bounds $x_{\min} \in \mathbb{R}$ and $x_{\max} \in \mathbb{R}$, i.e. $x_{\min} \leq x \leq x_{\max}$ by $\text{sat}(x_{\min}, x, x_{\max})$ which is defined as:

$$\text{sat}(x_{\min}, x, x_{\max}) = \begin{cases} x_{\max} & \text{if } x > x_{\max} \\ x & \text{if } x_{\min} \leq x \leq x_{\max} \\ x_{\min} & \text{if } x < x_{\min} \end{cases} \quad (1)$$

Similarly, for $x_{\min}, x, x_{\max} \in \mathbb{R}^n$, the saturation operator $\text{sat}(\cdot, \cdot, \cdot)$ can be applied to the vectors element-wise.

2.2 Power sharing and droop control

In islanded MGs, a balance between the local generation and consumption must be maintained at every time instant $k \in \mathbb{N}$. This can be captured by the algebraic power-balance equation

$$\mathbf{1}^\top p_t(k) + \mathbf{1}^\top p_s(k) + \mathbf{1}^\top p_r(k) + \mathbf{1}^\top w_d(k) = 0, \quad (2)$$

where $p_t(k) \in \mathbb{R}_{\geq 0}^{n_t}$, $p_s(k) \in \mathbb{R}^{n_s}$, $p_r(k) \in \mathbb{R}_{\geq 0}^{n_r}$ are power output of the conventional units, storage units and RES, respectively and $w_d(k) \in \mathbb{R}_{\leq 0}^{n_d}$ is the load demand. Here, $n_t, n_s, n_r, n_d \in \mathbb{N}$ denote the numbers of conventional units, storage units, renewable units and loads, respectively.

The power provided by the renewable units depends on the available renewable infeed $w_r(k) \in \mathbb{R}_{\geq 0}^{n_r}$ and the power setpoints $u_r(k) \in \mathbb{R}^{n_r}$, which set the maximum allowed infeed i.e.,

$$p_r(k) = \min(u_r(k), w_r(k)). \quad (3)$$

The uncertain load $w_d(k)$ and renewable infeed $p_r(k)$ can take unforeseen values. By design of the lower control layers, the grid-forming storage and conventional units automatically adjust their output power to ensure that (2) holds. This can be implemented, for example by using droop control which leads to a desired proportional power sharing (Krishna et al., 2017), (Schiffer et al., 2017). The share of each unit depends on the inverse droop gain, which we denote by $\chi_i \in \mathbb{R}$ which can be chosen, e.g., according to the nominal power of the units.

In EMS, which acts on a much slower time scale, it suffices to model droop control in a steady-state manner. To do so, consider an auxiliary free variable $\rho(k) \in \mathbb{R}$. This global variable describes the deviation of the system frequency from the nominal value. Assuming droop control at steady-state, the power of grid-forming units can be described by

$$p_t(k) = u_t(k) + \chi_t(k)\rho(k), \quad (4)$$

$$p_s(k) = u_s(k) + \chi_s(k)\rho(k) \quad (5)$$

where Here $u_t(k) \in \mathbb{R}^{n_t}$, $u_s(k) \in \mathbb{R}^{n_s}$ are the power setpoints, and $\chi_s \in \mathbb{R}_{\geq 0}^{n_s}$, $\chi_t \in \mathbb{R}_{\geq 0}^{n_t}$ are the inverse droop gain for the conventional units and the storage units.

2.3 Microgrid with saturation and droop control in all units

In this section, we will describe the model of the MG units while taking droop-control and saturation of the units into account. This includes a model of the low-level control which ensures that power and energy limit constraints are met.

Saturation in unit-level control: All units have physical limits that must be respected. Therefore, we consider saturation at the lower layers that enforces the operation range of a unit. For a unit i , with power p_i , saturation of its power is denoted by $\text{sat}(p_i^{\min}, p_i, p_i^{\max})$ which is defined as in (1).

Conventional generator: Conventional generators, such as diesel generators, usually serve as backup power sources. Typically, they operate as grid-forming units and participate in power sharing. They can be switched on or off, which is indicated by a vector of binary variables $\delta_t(k) \in \{0, 1\}^{n_t}$. If $\delta_{t,i}(k) = 0$, conventional unit $i \in \{1, \dots, n_t\}$ is switched off and its power is $p_{t,i}(k) = 0$ and it cannot participate in power sharing. If $\delta_{t,i}(k) = 1$, it is switched on and it participates in the power sharing. Thus, the power output can be represented as,

$$p_t(k) = \text{diag}(\delta_t(k)) \text{sat}(p_t^{\min}, u_t(k) + \chi_t \rho(k), p_t^{\max}). \quad (6)$$

By virtue of (6), we have that $p_t^{\min} \leq p_t(k) \leq p_t^{\max}$ is enforced through saturation.

Storage units: Storage units help to deal with the intermittency of renewable generation. Often, they are operated as grid-forming units. The dynamics of the storage units are

$$x(k) = x(k-1) - T_s p_s(k), \quad (7a)$$

where $T_s \in \mathbb{R}_{>0}$ is the sampling time. The energy storage capacities result in the constraints

$$x^{\min} \leq x(k) \leq x^{\max}, \quad (7b)$$

with $x^{\min} \in \mathbb{R}_{\leq 0}^{n_s}$ and $x^{\max} \in \mathbb{R}_{>0}^{n_s}$.

Storage operation is constrained by both power and energy limits. A straight forward and naive implementation of energy-based saturation would set the power to positive or negative value as soon as the energy hits the respective bound in (7b) using primary control. However, to avoid sudden power changes between sampling instances of the EMS, and to keep the analysis simple, we choose a different approach: Given the sampling time T_s and the current energy level x , we define time-varying admissible power bounds as

$$\begin{aligned} \bar{p}_s^{\min}(k) &= \max\left(p_s^{\min}, \frac{x(k-1) - x^{\max}}{T_s}\right), \\ \bar{p}_s^{\max}(k) &= \min\left(p_s^{\max}, \frac{x(k-1) - x^{\min}}{T_s}\right). \end{aligned} \quad (7c)$$

These time-varying power limits dynamically adjust the admissible power based on the current energy and sampling time, which prevents the storage energy from exceeding its limits. The power output of the storage subject to saturation at these limits can be represented as:

$$p_s(k) = \text{sat}(\bar{p}_s^{\min}(k), u_s(k) + \chi_s \rho(k), \bar{p}_s^{\max}(k)). \quad (7d)$$

Renewable units: We assume that the renewable units have droop control and outputs power of renewable units are curtailed at available power as seen in (3) and now additionally at the minimum power due to saturation. Therefore, their power output with saturation and droop control, can be expressed by

$$p_r(k) = \text{sat}(p_r^{\min}, u_r(k) + \chi_r \rho(k), w_r(k)), \quad (8)$$

where $u_r(k) \in \mathbb{R}^{n_r}$ are the power setpoints of renewable units, $\chi_r \in \mathbb{R}_{\geq 0}^R$ is the inverse droop gain for RES and

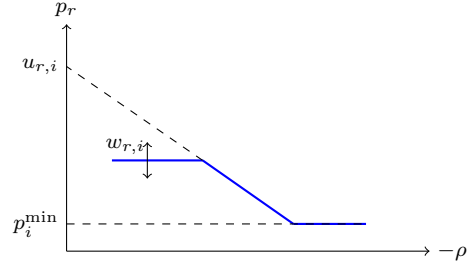


Fig. 1. A saturation-based droop-controlled RES unit i , with power setpoint $u_{r,i}$ and the available feed $w_{r,i}$.

p_r^{\min} is the minimum renewable power. Equation (8) can be visualised in Figure 1.

Remark 1. One can easily model units with no power sharing by setting $\chi_i = 0$, for $i \in \{1, \dots, n_t + n_s + n_r\}$.

Remark 2. In the saturation-based model, the power setpoint limits u^{\min} and u^{\max} for different units can differ from and even lie beyond the power limits. They can be chosen arbitrarily large.

3. PROBLEM FORMULATION

To address the uncertainties in RES and load in MG operation, we formulate a robust multi-scenario MPC problem. Unlike the minimax MPC strategy in (Hofmann et al., 2021), which relies on worst-case disturbance or uncertainty scenarios, and considers only the worst-case performance in the objective function. This can lead to suboptimal performance near the best-case disturbance scenarios. To mitigate this, we formulate a multi-scenario MPC problem that explicitly considers a range of possible scenario from worst-case to best-case, and integrates droop control and as well as physical limitation in all units through saturation. In this section, we define the uncertainty model and then describe in detail a multi-scenario optimal control problem.

3.1 Uncertainty model

Renewable generation and loads are represented as uncertain variables in the model. Here, uncertainty is modeled by lower and upper bounds. Compared to other approaches, e.g. stochastic ones, this formulation requires less information and significantly reduces the computational burden of the resulting control problem. The bounds of renewable generation and loads are obtained using a forecaster. At each future time step k , the forecaster is assumed to provide the corresponding upper and lower bounds such that

$$\underbrace{\begin{bmatrix} w_r^{\min}(k) \\ w_d^{\min}(k) \end{bmatrix}}_{w^{\min}(k)} \leq \underbrace{\begin{bmatrix} w_r(k) \\ w_d(k) \end{bmatrix}}_{w(k)} \leq \underbrace{\begin{bmatrix} w_r^{\max}(k) \\ w_d^{\max}(k) \end{bmatrix}}_{w^{\max}(k)}, \quad (9)$$

where $w_r^{\min}(k), w_r^{\max}(k) \in \mathbb{R}^{n_r}$ and $w_d^{\min}(k), w_d^{\max}(k) \in \mathbb{R}^{n_d}$ are the estimated upper and lower bounds of renewable generation and loads, respectively.

3.2 Operating cost

We consider an economically motivated operating cost associated with conventional units and the storage sys-

tems, assuming zero operating cost for RES. Conventional units' cost includes fuel cost with weight $C_t \in \mathbb{R}_{\geq 0}$, fixed generation cost with weight $C_{\text{on}} \in \mathbb{R}_{\geq 0}$ and switching cost with weight $C_{\text{sw}} \in \mathbb{R}_{\geq 0}$ and storage system cost with weight $C_s \in \mathbb{R}_{\geq 0}$. Let us denote the power outputs and power set points of the generation units at a given time instant $k \in \mathbb{N}$, by $p(k) = [p_t(k)^\top p_s(k)^\top p_r(k)^\top]^\top$ and, $u(k) = [u_t(k)^\top u_s(k)^\top u_r(k)^\top]^\top$, respectively. Thus, the total operation cost is

$$\ell(p(k), \delta_t(k), \delta_t(k-1)) = C_t^\top p_t(k) + C_{\text{on}}^\top \delta_t(k) + C_{\text{sw}}^\top |\delta_t(k) - \delta_t(k-1)| + C_s^\top p_s(k), \quad (10)$$

Note that, the storage unit cost defined as $C_s^\top p_s(k)$ is negative if power is stored, i.e., if $p_{s,i}(k) < 0$. This emphasises storing available RES power that cannot be consumed by load instantaneously.

3.3 Multi-scenario robust MPC

Let us consider the prediction horizon of the MPC as $N_p \in \mathbb{N}$. At sampling time instant k , the predicted power at future step $j \in N_p$ is given by $p(k+j|k)$. From now, we follow the convention that if a vector $z \in \mathbb{R}^{n_z}$, then $\mathbf{z} = [z(k+1) \ \cdots \ z(k+N_p)] \in \mathbb{R}^{n_z \times N_p}$. let us define the operation cost over the prediction horizon as

$$J(\mathbf{p}, \boldsymbol{\delta}_t, \delta_t(k)) := \sum_{j=1}^{N_p} \ell(p(k+j), \delta_t(k+j), \delta_t(k+j-1)). \quad (11)$$

The operation cost (11) can alternatively be written as $J(\mathbf{u}, \boldsymbol{\delta}_t, \delta_t(k), \mathbf{w})$ to explicitly specify the dependence on the control \mathbf{u} and the uncertainty \mathbf{w} . In the context of MPC, the question arises as to whether there is a control (over the prediction horizon) that is not only permissible in every scenario (i.e., satisfies the model equations and constraints) but is also optimal in every scenario.

With the notations defined above, this can be expressed mathematically as the following multi-scenario robust MPC problem.

Problem 1. (Multi-scenario robust MPC).

$$\min_{\mathbf{u}, \boldsymbol{\delta}_t} \max_{\mathbf{w}} \left(J(\mathbf{u}, \boldsymbol{\delta}_t, \delta_t(k), \mathbf{w}) - \min_{\mathbf{u}', \boldsymbol{\delta}_t'} J(\mathbf{u}', \boldsymbol{\delta}_t', \delta_t(k), \mathbf{w}) \right) \quad (12a)$$

subject to the model equations (2), (6), (7) and (8) where k is substituted by $k+j, \forall j \in \{1, \dots, N_p\}$, and control constraints are

$$\boldsymbol{\delta}_t \in \{0, 1\}^{n_t \times N_p}, \quad (12b)$$

$$\mathbf{u}^{\min} \leq \mathbf{u} \leq \mathbf{u}^{\max}, \quad (12c)$$

with initial conditions $x_s(k) = x_{s,0}$, $\delta_t(k) = \delta_{t,0}$, and $J(\cdot)$ is defined by (11), where, the constraints have to be satisfied for all $\mathbf{w} \in [\mathbf{w}^{\min}, \mathbf{w}^{\max}]$.

Problem 1 aims to minimize the cost across a set of pre-defined scenarios, represented by the uncertainty variable \mathbf{w} . First $\min_{\mathbf{u}'} J(\mathbf{u}', \boldsymbol{\delta}_t, \delta_t(k), \mathbf{w})$, the inner minimization problem, gives the best possible cost for a specific scenario \mathbf{w} . For each scenario, this gives a control $(\mathbf{u}^*, \boldsymbol{\delta}_t^*)$ which specifically minimizes the cost for that scenario, the result of which we can call scenario-specific optimal cost. In the second step, we are searching for one common

control $(\mathbf{u}, \boldsymbol{\delta}_t)$ which we actually implement (the decision of Problem 1). For a candidate $(\mathbf{u}, \boldsymbol{\delta}_t)$ we can apply this candidate to all the scenarios and for each scenario, study the difference between the resulting cost and previously calculated scenario-specific optimal cost. This difference is referred as the regret which tells us how much worse $(\mathbf{u}, \boldsymbol{\delta}_t)$ performs compared to the best possible $(\mathbf{u}^*, \boldsymbol{\delta}_t^*)$ for same scenario \mathbf{w} . This leads us to problem 1, where we want to minimize the maximum of these differences, i.e. the maximum regret. In particular, in this min-max problem, $\max_{\mathbf{w}}$ chooses the disturbance that makes the regret worst and $(\min_{\mathbf{u}, \boldsymbol{\delta}_t})$ aims to find the control $(\mathbf{u}^*, \boldsymbol{\delta}_t^*)$ which makes this worst-case regret as small as possible, and at best equal to zero. Therefore, clearly, if there exists a control $(\mathbf{u}^*, \boldsymbol{\delta}_t^*)$ which can optimize all scenarios simultaneously, then optimal cost for (12a) is zero can only be met under certain conditions. In the next section, we provide a more tractable operation control approach based on a rule-based determination of constant power setpoints \mathbf{u} and a unit commitment problem-based determination of switch states $\boldsymbol{\delta}_t$.

4. SOLUTION APPROACH WITH CONSTANT SETPOINTS AND UNIT COMMITMENT

In this section, we describe a rule based solution approach where at first, we provide a very simple rule-based control with the requirement that conventional units are always switched on. Then, we provide a robust MPC based EMS design which relaxes this condition by utilizing a unit-commitment approach to decide the switching of the conventional units.

4.1 Rule-based and saturation-based enforcement (constant setpoint calculation)

(Hofmann et al., 2021), previously considered a mini-max problem, where the worst-case cost (over all scenarios \mathbf{w}) is minimized, and where, like in Problem 1, the constraints have to be satisfied for all scenarios $\mathbf{w} \in [\mathbf{w}^{\min}, \mathbf{w}^{\max}]$. It was shown, that when unit power and energy saturation is enabled, the constraints can be equivalently stated by demanding that at any time and under any disturbance the instantaneous unit power saturation limits must allow that the power balance is satisfied. Furthermore, if the constraints are satisfied for \mathbf{w}^{\min} and \mathbf{w}^{\max} , then they are satisfied for all $\mathbf{w} \in [\mathbf{w}^{\min}, \mathbf{w}^{\max}]$. Here, we first consider the following requirements, which simplifies the problem by ensuring that the instantaneous unit power saturation limits are always guaranteed to allow the power balance to be satisfied.

- Requirement 1: All thermal generators are always switched on, $\delta_t = \mathbf{1}$.
- Requirement 2: The total load demand is never higher than the sum of the thermal generator upper saturation limits i.e. $\mathbf{1}^T w_d(k) \leq p_t^{\max}$.
- Requirement 3: The total load demand is never lower than the sum of the thermal generator lower saturation limits i.e. $p_t^{\min} \leq \mathbf{1}^T w_d(k)$.

As a result of these requirements, any given power setpoints $\mathbf{u} \in [u^{\min}, u^{\max}]$ are feasible, where u^{\min} and u^{\max}

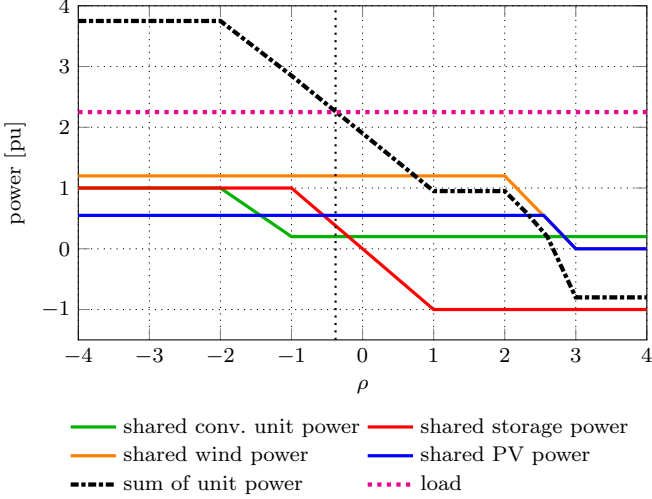


Fig. 2. Illustration of the rule-based configuration of the saturating droop functions.

can be chosen arbitrarily with $u^{\min} < u^{\max}$. The problem becomes effectively an unconstrained one.

For simplicity, we now assume that all thermal and storage cost factors are equal, so that $C_t^T = C_s^T =: C\mathbf{1}^T$. In the following, we determine a set of *constant* power setpoints $\mathbf{u} \in [u^{\min}, u^{\max}]$ with the aim of optimizing the cost function (11) under the above requirements. The resulting behavior can be achieved by a rule-based controller, which is realized through decentral saturating droop-control. It corresponds to the following prioritization:

- (1) use of renewables (if available) and charging the battery (if not full),
- (2) use of renewables (if available) and discharging the battery (if not empty),
- (3) use of renewables (if available) and discharging the battery (if not empty) and use of thermal generators.

The saturating frequency-droop-curves for units are illustrated in Figure 2. For large frequency deviations ρ , all units are in lower saturation. For low ρ values, units are in upper saturation. For the prioritization to be realized by saturating droop curves, it is essential that the linear droop regions of the unit types are always non-overlapping. This must hold for values of the saturation limits, which can depend on available power of renewables and the state of charge (SOC) of storage units) non-overlapping.

Proposition 1. Provided that u^{\min} is sufficiently low and u^{\max} , respectively high, even outside of $[p^{\min}, p^{\max}]$, appropriate power set-points u^* can be calculated according to

$$u_t^* = p_t^{\min} - \rho_s^{\max} \chi_t \quad (13a)$$

$$u_r^* = p_r^{\max} - \rho_s^{\min} \chi_r \quad (13b)$$

$$u_s^* = 0 \quad (13c)$$

where,

$$\rho_s^{\min} = \min_i \left(\frac{p_{s,i}^{\min}}{\chi_{s,i}} \right) \quad (13d)$$

$$\rho_s^{\max} = \max_i \left(\frac{p_{s,i}^{\max}}{\chi_{s,i}} \right) \quad (13e)$$

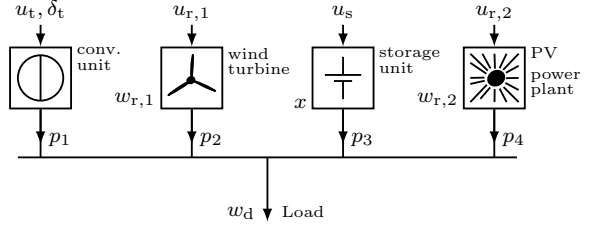


Fig. 3. Microgrid topology with a conventional generator, a wind turbine, a storage unit, a PV power plant and a load.

Proof: Let us define infeed energies between time step $k + j$ and $k + N_p$:

$$x_t(j \rightarrow N_p) := T_s \sum_{j=1}^{N_p} p_t(k + j), \quad (14a)$$

$$x_r(j \rightarrow N_p) := T_s \sum_{j=1}^{N_p} p_r(k + j). \quad (14b)$$

The cost (11) can also be expressed as (shifted by a fixed part depending on initial stored energy):

$$\tilde{J} := J - \frac{C}{T_s} x(k) = \frac{C}{T_s} (x_t(1 \rightarrow N_p) - x(k + N_p)). \quad (15)$$

Consider the last time segment ($k + N_p - 1 \rightarrow k + N_p$), and the associated cost $\tilde{J}(N_p - 1 \rightarrow N_p) = \frac{C}{T_s} (x_t(N_p - 1 \rightarrow N_p) - x(k + N_p))$. It can be shown that, for any $w(k + N_p - 1)$ and $x(k + N_p - 1)$, (13) is an optimal control for the one-timestep-problem of minimizing $\tilde{J}(N_p - 1 \rightarrow N_p)$, and we denote the minimum cost as $\tilde{J}^*(N_p - 1 \rightarrow N_p)$. In order to continue the proof by induction, the effect of a variation of $x(k + N_p - 1)$ on $\tilde{J}^*(N_p - 1 \rightarrow N_p)$ can be studied. Because the optimal control of the last time segment is independent of $x(k + N_p - 1)$, this just means that the effect of this initial condition variation on the result of a known control has to be studied. We can make use of derivations given in Hofmann et al. (2021). If $x^{(2)}(k + N_p - 1) \geq x^{(1)}(k + N_p - 1)$, then

$$p_t^{(2)}(k + N_p - 1) \leq p_t^{(1)}(k + N_p - 1), \quad (16a)$$

$$p_r^{(2)}(k + N_p - 1) \leq p_r^{(1)}(k + N_p - 1), \quad (16b)$$

$$x^{(2)}(k + N_p) \geq x^{(1)}(k + N_p), \quad (16c)$$

which means

$$x_t^{(2)}(N_p - 1 \rightarrow N_p) \leq x_t^{(1)}(N_p - 1 \rightarrow N_p), \quad (17a)$$

$$x_r^{(2)}(N_p - 1 \rightarrow N_p) \leq x_r^{(1)}(N_p - 1 \rightarrow N_p). \quad (17b)$$

An energy balance over the last time segment results in (load demand is fixed and cancels out):

$$\begin{aligned} & x_t^{(2)}(N_p - 1 \rightarrow N_p) - x_t^{(1)}(N_p - 1 \rightarrow N_p) + \\ & x_r^{(2)}(N_p - 1 \rightarrow N_p) - x_r^{(1)}(N_p - 1 \rightarrow N_p) + \\ & x^{(2)}(k + N_p - 1) - x^{(1)}(k + N_p - 1) - \\ & (x^{(2)}(k + N_p) - x^{(1)}(k + N_p)) = 0. \end{aligned} \quad (18)$$

So that

$$\begin{aligned} & \frac{T_s}{C} (\tilde{J}^{(2)*}(N_p - 1 \rightarrow N_p) - \tilde{J}^{(1)*}(N_p - 1 \rightarrow N_p)) = \\ & (x_t^{(2)}(N_p - 1 \rightarrow N_p) - x^{(2)}(k + N_p)) - \\ & (x_t^{(1)}(N_p - 1 \rightarrow N_p) - x^{(1)}(k + N_p)) = \\ & - (x^{(2)}(k + N_p - 1) - x^{(1)}(k + N_p - 1)) + \\ & x_r^{(1)}(N_p - 1 \rightarrow N_p) - x_r^{(2)}(N_p - 1 \rightarrow N_p) \geq \\ & - (x^{(2)}(k + N_p - 1) - x^{(1)}(k + N_p - 1)). \end{aligned} \quad (19)$$

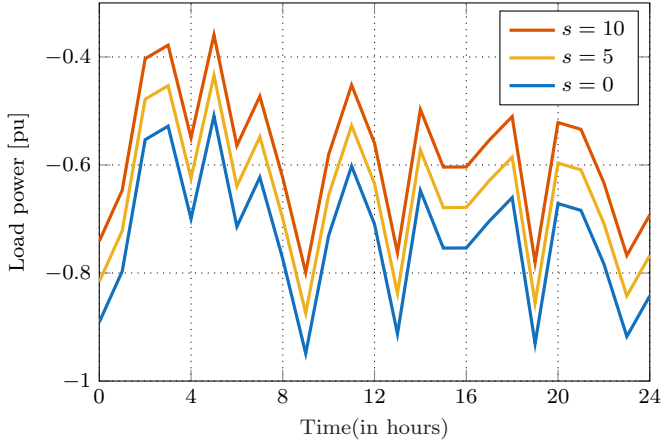


Fig. 4. Load demand profiles w_d^s for different scenarios (s) for day 1 in the case study.

The cost reduction, for time segment $k + N_p - 1 \rightarrow k + N_p$, achievable by increasing the stored energy at $k + N_p - 1$ by $(x^{(2)}(k + N_p - 1) - x^{(1)}(k + N_p - 1))$ is thus limited by $\frac{C}{T_s}(x^{(2)}(k + N_p - 1) - x^{(1)}(k + N_p - 1))$. With this information, the optimal control (13) can be confirmed also for time segment $k + N_p - 2 \rightarrow k + N_p - 1$, and inductively for the entire prediction horizon.

4.2 Simplified EMS with constant setpoints and unit commitment problem

For calculating optimal constant power setpoints u^* in the previous section, it was assumed that the thermal generators are uncontrollable and always on. In the following, we propose a heuristic solution to the original Problem 1. The calculated constant power setpoints are implemented, and an outer mini-max MPC-problem is posed to determine optimal thermal generator switch states. The aim is to switch on thermal generators only as long as necessary to robustly satisfy the constraints (i.e., allow the power balance to be satisfied) and to minimize the worst-case cost $\max_{\mathbf{w}} J(u^*, \delta_t, \delta_t(k), \mathbf{w})$. This is a unit commitment problem and can be stated as:

Problem 2. (Saturating droop unit commitment EMS).

$$\min_{\delta_t} \max_{\mathbf{w}} J(u^*, \delta_t, \delta_t(k), \mathbf{w}), \quad (20)$$

subject to the model equations (2), (6), (7) and (8) and control constraints (13) with initial conditions $x_s(k) = x_{s,0}$, $\delta_t(k) = \delta_{t,0}$, and $J(\cdot)$ is defined by (11).

5. CASE STUDY

In this section, we present a case study evaluating the performance of the proposed EMS in Problem 2, on a MG with high renewable share as shown in Figure 3. In this case study, we also compare its performance with a prescient controller and the minimax robust MPC from (Hofmann et al., 2021). The following subsections detail the microgrid configuration and prescient MPC followed by implementation, simulation results and discussions.

5.1 Simulation setup

For performance evaluation and comparison we consider the MG depicted in Figure 3. It consists of a conventional

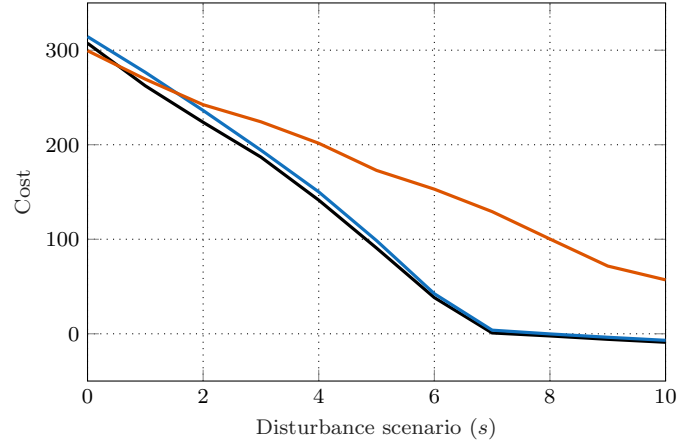


Fig. 5. Comparison of the closed-loop cost calculated over one week simulation, for different controllers and different disturbance scenarios. Scenario s is on the x-axis and the total cost is on y-axis.

generator, a wind turbine, a storage unit, a PV power plant and a load. Table 1 lists the power and energy limits of the units along with the droop gains and weights used in the cost function. Note that C_s is smaller than C_t to discourage charging the storage with conventional power. The EMS sampling time is 15 min and the prediction horizon of the MPC is 8 h, i.e., $N_p = 32$. The simulation horizon is 7 days, i.e., $N_s = 672$. The model and the controllers are implemented in Matlab[®]2022b. The MPC optimization is formulated using YALMIP (Löfberg, 2004) and solved with Gurobi 11.0.0 (Gurobi Optimization LLC, 2025).

5.2 A prescient controller

A prescient MPC controller is a hypothetical controller which has perfect future knowledge of the available renewable infeed and the load demand denoted w^{actual} . In this case, the uncertainty model (9) is substituted by $\mathbf{w}^{\min} = \mathbf{w}^{\max} = \mathbf{w}^{\text{actual}}$, effectively the multiscenario robust MPC in (12a) is converted to a single-scenario ($\mathbf{w}^{\text{actual}}$).

Table 1. Unit parameters and weights of cost function.

Parameter	Value	Weight	Value
$[u_t^{\min} u_s^{\min} u_{r,1}^{\min} u_{r,2}^{\min}]$	$[-5 \ -5 \ -5 \ -5]$ pu	C_t	1
$[u_t^{\max} u_s^{\max} u_{r,1}^{\max} u_{r,2}^{\max}]$	$[5 \ 5 \ 5 \ 5]$ pu	C_{on}	0.2
$[p_t^{\min} p_s^{\min} p_{r,1}^{\min} p_{r,2}^{\min}]$	$[0.2 \ -1 \ 0 \ 0]$ pu	C_{sw}	0.3
$[p_t^{\max} p_s^{\max}]$	$[1 \ 1]$ pu	C_s	0.9
$[x_{\min} x_{\max}]$	$[0 \ 6]$ pu h	$\delta_{t,0}$	0
x^0	2 pu h		
$[\chi_t \ \chi_s \ \chi_{r,1} \ \chi_{r,2}]$	$[1 \ 1 \ 1 \ 1]$		

5.3 Closed-loop comparison

In this section, closed-loop simulations with different MPC controllers are performed over a 7-day period, comprising

$N_s = 672$ sampling instances and for 11 disturbance scenarios. Recall from (9), since power consumption w_d is negative, the worst-case scenario \mathbf{w}^{\min} occurs when we have minimum available renewable power and maximum absolute value of power consumption and the best-case scenario \mathbf{w}^{\max} occurs, when there is maximum renewable available power and minimum absolute value power consumption. We create the 11 scenarios using linear interpolation between the worst-case scenario profile and the best-case scenario profile:

$$w^s(k) = w^{\min}(k) + \alpha_s(w^{\max}(k) - w^{\min}(k)), \forall k \quad (21)$$

where, $\alpha_s \in [0, 1]$ such that $\alpha_s = 0.1s$, for $s \in \{0, \dots, 10\}$.

As an example, Figure 4 shows scenarios of w_d^s for $s = 0, 5$ and 10 . Based on the total operation cost (10), (11), the total cost is calculated over the entire $N_s = 672$ samples by

$$J^{\text{closed-loop}} := \sum_{k=1}^{N_s} \ell(p(k), \delta_t(k), \delta_t(k-1)), \quad (22)$$

where the models parameters are listed in Table 1.

Figure 5 depicts the total cost associated with different controllers, for each scenario defined in (21).

It can be seen from Figure 5 that the rule-based controller including thermal generator unit commitment, Problem 2, achieves almost the same performance as the prescient controller in all scenarios and more so when we move towards the best-case scenario. In addition, it also clearly outperforms the minimax MPC from (Hofmann et al., 2021), as soon as we go away from the worst-case scenarios. This results from the combination of the prioritizing constant power setpoints, which are always optimal when the thermal generator is fixed on or off all the time, and the ability to schedule the thermal generator on a robust MPC-basis. The observed slight performance gap could be explained as follows: the scheduling involves both on and off phases, and it turns out that the chosen constant setpoints are no longer optimal during an on-phase. This is due to the thermal generator fixed on-cost and the switching cost, which would make it worthwhile to reduce the necessary on-time. A required total amount of energy could be produced in a shorter time, stored in the storage units and retrieved later.

6. CONCLUSION

In this paper, we have presented a novel hierarchical control strategy for islanded microgrids. On the primary control layer, droop control of conventional and renewable units is considered, which also includes autonomous power and energy limiting. We have shown that appropriately chosen constant power setpoints can correspond to an optimal control under certain conditions. This primary control strategy is combined with a robust MPC-based energy management system, which decides the unit commitment of conventional units. The main aim of this design is to enhance operating cost under a wide range of scenarios regarding uncertain inputs such as load demand and available renewable power. In a case study, we have demonstrated that the proposed hierarchical control clearly outperforms previous robust energy management schemes. Given the relative simplicity of the approach in its present form, we suggest that it can be specially well suited for small-scale microgrids. In future work, we

intend to enhance the design by using a robust EMS which provides minimum energy setpoints to the primary layer, relax system requirements and provide corresponding theoretical guarantees.

7. ACKNOWLEDGEMENT

The authors thank Christian A. Hans for valuable comments and helpful discussions.

REFERENCES

- Baekeland, N., Chatterjee, D., Lu, M., Johnson, B., and Seo, G.S. (2024). Overcurrent limiting in grid-forming inverters: A comprehensive review and discussion. *IEEE Transactions on Power Electronics*, 39(11), 14493–14517.
- Dörfler, F., Simpson-Porco, J.W., and Bullo, F. (2016). Breaking the hierarchy: Distributed control and economic optimality in microgrids. *IEEE Transactions on Control of Network Systems*, 3(3), 241–253.
- Du, W. and Lasseter, R.H. (2017). Overload mitigation control of droop-controlled grid-forming sources in a microgrid. In *2017 IEEE Power & Energy Society General Meeting*, 1–5.
- Gao, X., Zhou, D., Anvari-Moghaddam, A., and Blaabjerg, F. (2025). Seamless switching method between grid-following and grid-forming control for renewable energy conversion systems. *IEEE Transactions on Industry Applications*, 61(1), 597–606.
- Guerrero, J.M., Vasquez, J.C., Matas, J., de Vicuna, L.G., and Castilla, M. (2011). Hierarchical control of droop-controlled ac and dc microgrids—a general approach toward standardization. *IEEE Transactions on Industrial Electronics*, 58(1), 158–172.
- Gurobi Optimization LLC (2025). Gurobi optimizer reference manual. URL <https://www.gurobi.com>.
- Hans, C.A., Nenchev, V., Raisch, J., and Reincke-Collon, C. (2014). Minimax model predictive operation control of microgrids. *IFAC Proceedings Volumes*, 47(3), 10287–10292. doi:10.3182/20140824-6-za-1003.00683. 19th IFAC World Congress.
- Hofmann, S., Sampathirao, A.K., Hans, C.A., Raisch, J., Heidt, A., and Bosch, E. (2021). Saturation-aware model predictive energy management for droop-controlled islanded microgrids. URL <https://arxiv.org/abs/2107.02719>.
- Khan, M., Wu, W., and Li, L. (2024). Grid-forming control for inverter-based resources in power systems: A review on its operation, system stability, and prospective. *IET Renewable Power Generation*, 18(6), 887–907.
- Krishna, A., Hans, C.A., Schiffer, J., Raisch, J., and Kral, T. (2017). Steady state evaluation of distributed secondary frequency control strategies for microgrids in the presence of clock drifts. In *2017 25th Mediterranean Conference on Control and Automation (MED)*, 508–515.
- Löfberg, J. (2004). YALMIP : a toolbox for modeling and optimization in MATLAB. In *2004 IEEE International Symposium on Computer Aided Control Systems Design*, 284–289. doi:10.1109/cacsd.2004.1393890.
- Olivares, D.E., Mehrizi-Sani, A., Etemadi, A.H., Cañizares, C.A., Iravani, R., Kazerani, M., Hajimiragha,

- A.H., Gomis-Bellmunt, O., Saeedifard, M., Palma-Behnke, R., Jiménez-Estévez, G.A., and Hatziaargyriou, N.D. (2014). Trends in microgrid control. *IEEE Transactions on Smart Grid*, 5(4), 1905–1919.
- Parisio, A., Rikos, E., and Glielmo, L. (2014). A model predictive control approach to microgrid operation optimization. *IEEE Trans. Control Syst. Technol.*, 22(5), 1813–1827. doi:10.1109/tcst.2013.2295737.
- Rocabert, J., Luna, A., Blaabjerg, F., and Rodríguez, P. (2012). Control of power converters in ac microgrids. *IEEE Transactions on Power Electronics*, 27(11), 4734–4749.
- Schiffer, J., Hans, C.A., Kral, T., Ortega, R., and Raisch, J. (2017). Modeling, analysis, and experimental validation of clock drift effects in low-inertia power systems. *IEEE Transactions on Industrial Electronics*, 64(7), 5942–5951.
- Schiffer, J., Zonetti, D., Ortega, R., Stanković, A.M., Sezi, T., and Raisch, J. (2016). A survey on modeling of microgrids—from fundamental physics to phasors and voltage sources. *Automatica*, 74, 135–150.
- Yazdani, S., Ferdowsi, M., Davari, M., and Shamsi, P. (2020). Advanced current-limiting and power-sharing control in a pv-based grid-forming inverter under unbalanced grid conditions. *IEEE Journal of Emerging and Selected Topics in Power Electronics*, 8(2), 1084–1096.